HHS Public Access

Author manuscript

Int J Radiat Oncol Biol Phys. Author manuscript; available in PMC 2023 March 01.

Published in final edited form as:

Int J Radiat Oncol Biol Phys. 2022 March 01; 112(3): 759–770. doi:10.1016/j.ijrobp.2021.09.039.

Therapeutic Intervention Using a Smad7-Based Tat Protein to Treat Radiation-Induced Oral Mucositis

Mary-Keara Boss, DVM, PhD[*], **Yao Ke, DDS, PhD**[†], **Li Bian, MD, PhD**[†,‡], **Lauren G. Harrison, BS**[*], **Ber-In Lee, DVM**[*], **Amber Prebble, BA**[*], **Tiffany Martin, DVM**[*], **Erin Trageser, DVM**[*], **Spencer Hall, BS**[†,‡], **Donna D. Wang, BS**[†,‡], **Suyan Wang, MS**[†,‡], **Lyndah Chow, MS**[§], **Barry Holwerda, PhD**[‖], **David Raben, MD**[¶], **Daniel Regan, DVM, PhD**[#], **Sana D. Karam, MD, PhD**[¶], **Steven Dow, DVM, PhD**[§], **Christian D. Young, PhD**[†,‡], **Xiao-Jing Wang, MD, PhD**[†,‡]

[*]Department of Environmental and Radiological Health Sciences, Colorado State University, Fort Collins, Colorado

[†]Department of Pathology, University of Colorado Anschutz Medical Campus, Aurora, Colorado

[‡]Allander Biotechnologies, LLC, Aurora, Colorado

[§]Department of Clinical Sciences, Colorado State University, Fort Collins, Colorado

[‖]Mtibio, Las Vegas, Nevada

[¶]Department of Radiation Oncology, University of Colorado Anschutz Medical Campus, Aurora, Colorado

[#]Department of Microbiology, Immunology and Pathology, Colorado State University, Fort Collins, Colorado

Abstract

Purpose: Recent studies reported therapeutic effects of Smad7 on oral mucositis in mice without compromising radiation therapy–induced cancer cell killing in neighboring oral cancer. This study aims to assess whether a Smad7-based biologic can treat oral mucositis in a clinically relevant setting by establishing an oral mucositis model in dogs and analyzing molecular targets.

Methods and Materials: We created a truncated human Smad7 protein fused with the cell-penetrating Tat tag (Tat-PYC-Smad7). We used intensity modulated radiation therapy to induce oral mucositis in dogs and applied Tat-PYC-Smad7 to the oral mucosa in dose-finding studies after intensity modulated radiation therapy. Clinical outcomes were evaluated. Molecular targets were analyzed in biopsies and serum samples.

Corresponding authors: Christian D. Young, PhD, Mary-Keara Boss, DVM, PhD and Xiao-Jing Wang, MD, PhD; Keara.Boss@colostate.edu, Christian.Young@allanderbiotech.com, xj.wang@cuanschutz.edu.
Mary-Keara Boss and Yao Ke contributed equally to this publication.
Li Bian is currently at the Department of Pathology, the First Affiliated Hospital of Kunming Medical University, Kunming, P.R. China.

Disclosures: X.J.W. is an inventor of the patent filed by the University of Colorado for using Tat-Smad7 to treat oral mucositis. Allander Biotechnologies, LLC, has the exclusive license and commercial interests in developing Smad7-based therapy.

All data generated and analyzed during this study are included in this article and its associated supplementary information files. Supplementary material associated with this article can be found, in the online version, at doi:10.1016/j.ijrobp.2021.09.039.

Results: Tat-PYC-Smad7 treatment significantly shortened the duration of grade 3 oral mucositis based on double-blinded Veterinary Radiation Therapy Oncology Group scores and histopathology evaluations. Topically applied Tat-PYC-Smad7 primarily penetrated epithelial cells and was undetectable in serum. NanoString nCounter Canine IO Panel identified that, compared to the vehicle samples, top molecular changes in Tat-PYC-Smad7 treated samples include reductions in inflammation and cell death and increases in cell growth and DNA repair. Consistently, immunostaining shows that Tat-PYC-Smad7 reduced DNA damage and neutrophil infiltration with attenuated TGF-β and NFκB signaling. Furthermore, IL-1β and TNF-α were lower in Tat-PYC-Smad7 treated mucosa and serum samples compared to those in vehicle controls.

Conclusions: Topical Tat-PYC-Smad7 application demonstrated therapeutic effects on oral mucositis induced by intensity modulated radiation therapy in dogs. The local effects of Tat-PYC-Smad7 targeted molecules involved in oral mucositis pathogenesis as well as reduced systemic inflammatory cytokines.

Oral mucositis, painful ulceration of the oral mucosa, is a common toxic effect of radiation therapy (RT) for bone marrow transplant, craniofacial RT for head and neck cancer (HNC), and chemo-RT for all cancer types.[1] Approximately 70% of HNC patients develop oral mucositis during treatment, which can be severe enough to cause reduction in oral intake or premature withdrawal from cancer treatment.[1,2] Similarly, canine cancer patients undergoing craniofacial RT develop oral mucositis with a rate and kinetics similar to human patients.[3–5] Intensity modulated RT (IMRT) and stereotactic body RT are increasingly used to precisely target cancer lesions and spare more normal tissue in both human and veterinary oncology clinics. However, these treatments do not reduce acute toxicity in the oral mucosa of HNC patients[6] because neighboring mucosa is still exposed to high-intensity radiation, albeit at a lower dose than the cancer. Furthermore, certain patients are at a high risk for oral mucositis regardless of treatment regimen.[7]

Palifermin, recombinant human keratinocyte growth factor, is the only Food and Drug Administration–approved targeted therapy for preventing oral mucositis in bone marrow transplant patients (4% of the at-risk population), but it has no effect on existing mucositis.[8] Currently, there is no Food and Drug Administration–approved drug to treat oral mucositis in cancer patients. These facts highlight the urgent need for therapeutic intervention, but the lack of a clinically applicable model capturing the complex oral mucositis pathogenesis[9] has hindered screening of therapeutic interventions. To this end, the current study sought to develop an IMRT-induced oral mucositis canine model because RT-induced oral mucositis in HNC treatment in dogs is similar to that in human cancer patients.[3,10] Additionally, the canine oral mucosa is remarkably similar to human oral mucosa.[11]

With respect to ongoing therapeutic interventions in humans, clinical trials of palifermin in oral cancer patients showed modest prevention of severe oral mucositis,[12,13] but it is not approved to treat oral mucositis in cancer patients. Clinical trials for GC4419, a superoxide dismutase mimetic, to treat oral mucositis in HNC patients revealed reductions in severe oral mucositis cases.[14] GC4419 requires intravenous infusions corresponding to the first 14 doses of RT. Because it is difficult to predict which patients will develop severe oral mucositis,

we sought to develop a therapeutic intervention that is topically applied to oral mucosa once RT-induced damage begins and targets multiple pathogenic processes of oral mucositis.

Previous work demonstrated that in addition to NFκB activation, activated transforming growth factor β (TGF-β) signaling contributes greatly to radiation-induced oral mucositis.[15] TGF-β is a potent growth inhibitor and apoptosis inducer for epithelial cells and a proinflammatory cytokine in oral mucosa.[16] To dampen both TGF-β and NFκB pathways to treat oral mucositis, we developed a recombinant Smad7 protein that contains human Smad7 fused to the HIV-1 Tat protein transduction domain. Tat-Smad7 protein rapidly penetrates cells upon contact.[15] Local delivery of Tat-Smad7 to mouse oral mucosa shows prophylactic and therapeutic effects on radiation-induced oral mucositis with increases in survival, migration, and DNA damage repair of normal oral keratinocytes but not HNC cells in vitro or in vivo.[15,17] In contrast, administration of an irrelevant Tat-conjugated protein did not have any effect on oral mucositis, suggesting that Tat-Smad7's effects on oral mucositis are specifically linked to Smad7 functions.[15] Furthermore, using the same oral mucositis model in mice, palifermin prevented development of oral mucositis, but it was not effective in treating oral mucositis once it developed, in contrast to the effective Tat-Smad7 treatment.[15] Given that the anti-TGF-β, anti-NFκB, and DNA damage repair functions of Smad7 are primarily attributed to the PY domain and the MH2 domain,[18,19] we sought to test whether a truncated Smad7-based Tat protein that retains these functions (ie, Tat-PYC-Smad7 without its MH1 domain) is sufficient to yield a therapeutic effect on oral mucositis in a radiation oncology setting. Here we show that we successfully established an IMRT-induced oral mucositis model in dogs and provide evidence that topical Tat-PYC-Smad7 application alleviated oral mucositis by directly targeting local pathogenic factors in the lesion and their secretions into the bloodstream.

Methods and Materials

Generation and formulation of Tat-PYC-Smad7

We produced recombinant Tat-tagged protein containing amino acids 203–426 of human Smad7 (Tat-PYC-Smad7) as a GST fusion protein in *Escherichia coli*, similarly to previously described methods.[15] Tat-PYC-Smad7 was cleaved from GST with PreScission protease followed by either size exclusion chromatography or heparin affinity chromatography to purify Tat-PYC-Smad7 protein as a monomer (Fig. E1). We used hydroxypropyl cellulose (HPC) gel (1% Klucel HF, Ashland) containing 1 × phosphate-buffered saline (PBS) and 15% glycerol as the base of the oral gel. We formulated Tat-PYC-Smad7 oral gel by mixing a 1:2 ratio of the protein stock with the base gel.

IMRT-induced oral mucositis in dogs

We enrolled 10 experimental beagles under the IACUC at Colorado State University (CSU). After completion of the study, dogs were adopted. The clinical protocol is included in Figure E2. This study used both sexes, and dogs were between 2.5 and 4 years old. Before RT, standard laboratory assessments (complete blood count, biochemistry panel, urinalysis) and a full physical examination were performed. A 6-mm pretreatment biopsy from the IMRT mapped area was performed. Each dog received IMRT irradiation daily for 5 days in week

1. We initially tested 4 to 6 Gy × 5 fractions (20–30 Gy) (600 cGy/min) to the maxilla (with exception of 1 mandible mucosa) in the region extending from the incisors to the caudal aspect of the canine teeth and selected 5 Gy × 5 (25 Gy) to maxillary mucosa for treatment. The total irradiated area is about 23.1 cm^2 (range, 20.6–38.1 cm^2).

Tat-PYC-Smad7 treatment

In weeks 2 and 3 after initial RT, dogs were treated with HPC gel (vehicle, “mock gel”) on 1 lateral site (11.6 cm^2) and Tat-PYC-Smad7 (drug, 0.5–8 μg daily dose) on the adjacent lateral site (11.6 cm^2) of the irradiated area, divided by a ~5 mm to 10 mm dental mold; sites were randomly alternated for vehicle and drug among dogs. Each dog was under anesthesia during treatment, induced with midazolam (0.2 mg/kg) and propofol (3 mg/kg) and maintained on isoflurane gas (to effect). Dogs were in a dorsal recumbent position, with the 2 sides separated by a divider mold. The dog was angled toward the treatment side during application, and the muzzle was gently taped to ensure the topical treatment stayed within the irradiated field. Each side was exposed to 0.5 mL HPC gel with or without drug for 30 minutes under anesthesia, allowing natural draining of the gel afterward. Because it is difficult to determine the crossover amount of a drug to the adjacent vehicle side, the drug-treated site was used to evaluate pharmacodynamics markers. This set-up allowed us to perform double-blind treatment and histopathology evaluation. Dogs recovered from anesthesia without food or water intake for 1 hour after treatment.

Evaluation of oral mucositis severity

Gross appearance of oral mucositis was scored daily based on Veterinary Radiation Therapy Oncology Group (VRTOG) criteria, and general health was monitored. At the time of development of grade 3 mucositis, dogs were treated with gabapentin (5–10 mg/kg orally every 8–12 hours) with or without amantadine (2–3.5 mg/kg orally every 24 hours). Full physical examinations were performed daily until the VRTOG score returned to 0, typically at the end of week 4. Posttreatment biopsy was performed 30 minutes after the last drug treatment on week 3. Posttreatment biopsies were fixed in 10% formalin, embedded in paraffin, and cut in 5 μm sections. Histology of hematoxylin and eosin–stained slides was performed independently by 2 treatment-blinded pathologists.

NanoString nCounter Canine IO Panel analysis

RNA was harvested from formalin fixed, paraffin embedded (FFPE) maxillary posttreatment biopsy samples using Qiagen RNeasy FFPE kit following the manufacturer’s instructions. RNA was quantified by NanoDrop spectrophotometry, and integrity was evaluated by Agilent TapeStation at the Colorado Molecular Correlates Laboratory. Integrity scores (RIN values) were extremely poor, as expected from FFPE-harvested RNA, but all samples had >50% RNA of 200 nucleotides or larger, making them suitable for analysis by NanoString nCounter analysis, which demonstrates 0.87 to 0.90 correlation comparing high-quality RNA from fresh frozen tissue versus matched low-quality RNA from FFPE tissue.[20,21] The only NanoString gene panel available for canine RNA is the nCounter Canine IO Panel, but this panel includes 800 genes, including many genes encoding cytokines, chemokines, DNA damage repair factors, and inflammatory response factors that play critical roles in both cancer and oral mucositis. Due to low abundance, 30 ng RNA was hybridized to

the NanoString nCounter Canine IO codeset/probeset for 24 hours at 65°C, then loaded to a nCounter Sprint Cartridge and analyzed on a nCounter SPRINT Profiler. nSolver 4.0 software was used to evaluate data quality, normalize raw count data to the geometric mean of 20 reference genes, and export normalized count data. Imaging and data contained no quality control flags. Normalized count data for all 800 genes in all 12 samples are provided in Table E1.

For each gene, the average normalized count of 6 Tat-PYC-Smad7 treated samples was divided by the average normalized count of the 6 mock gel treated samples to determine the fold change in gene expression in Tat-PYC-Smad7 treated samples. The difference was considered significant if $P < .05$ as determined by 2-tail Student's t test. Nanostring divides this 800-gene panel into 27 functional categories, and we generated a 28th category that only included the secreted cytokines and chemokines in a "secreted cytokine and chemokine signaling" category (Fig. E3). Normalized gene count data and these 28 gene sets (Table E2) were evaluated by gene set enrichment analysis using desktop software version 4.1.0.

Immunohistochemistry

We performed immunohistochemistry (IHC) staining as previously described.[15] Primary antibodies used were rabbit anti-Ki67 (1:500) (Cell Signaling Technology, 12202), rabbit anti-NFκB-p105/p50 [p Ser337] (1:300) (Novus Biologicals, NB100–82074), rabbit anti-pSmad3 (1:400, Abcam, ab52903), rabbit anti-pH2AX (1:100) (Cell Signaling Technology, 9718), rabbit anti-myeloperoxidase (Ready-to-Use, Dako, GA51161–2), rabbit anti-hemagglutinin (HA) (1:700) (Cell Signaling Technology, 3724), rabbit anti-IL-1β (1:500) (Novus Biologicals, NB600–633), rabbit anti-TNF-α (1:200) (Novus Biologicals, NBP1–19532), mouse anti-CCL2 (1:50) (Novus Biologicals, MAB28171), and goat anti-IL-6 (1:40) (R&D, AF1609) antibodies. Nuclear pSmad3-, NFκB p50-, or pH2AX-positive cells were quantified as the percent of positive cells per total epithelial cell count (excluding sloughed epithelial cells induced by irradiation). Nuclear Ki67 was quantified as positive cells per length of basement membrane. For pH2AX staining, cells with more than 3 nuclear foci were defined as pH2AX-positive cells. Myeloperoxidase-positive cells were quantified per square millimeter epithelial and stroma area above the muscle layer, and sequential 10 × images along the basement membrane were quantified and averaged per sample using Olympus cellSens Dimension software.

Cytokine Luminex assay to detect serum cytokines

MILLIPLEX Canine Cytokine/Chemokine Magnetic Bead Panel-Immunology Multiplex Assay (MilliporeSigma CCYTMG-90K-PX13), which detects TNF-α, IL-6, CCL2, IL-8, and IL-10, was used to detect serum levels of these cytokines. We used 50 μL serum. Serum levels of IL-1β were detected using enzyme-linked immunosorbent assay (ELISA) (Duoset for canines) (R&D #DY3747) according to the manufacturer's protocol; 100 μL serum per dog was used for detection.

ELISA to detect systemic Tat-PYC-Smad7 from local application

We generated a sandwich ELISA to detect Tat-PYC-SMAD7 because no commercially available sandwich ELISA that we tried was able to detect Tat-PYC-SMAD7. Rabbit anti-

Smad7 (Novus NBP1–87728) was coated onto 96-well plates (Nunc-Immuno #446612) overnight and served to capture Smad7. Mouse monoclonal antibody (R&D #MAB2029) that recognizes the c-terminus of human SMAD7 was used for detection. We used HRP-conjugated horse anti-mouse-IgG (Cell Signaling Technologies) to detect captured immune complexes and 1-Step Ultra TMB-ELISA substrate (Thermo) to detect HRP activity, followed by acid quenching and detection on a plate reader at 450 nm. We spiked Tat-PYC-Smad7 into untreated dog serum to establish a standard curve and compared Smad7 levels in dog serum samples before and after Tat-PYC-Smad7 treatment for 2 weeks, with the last treatment 30 minutes before serum was collected.

Anti-drug antibody ELISA

Tat-PYC-Smad7 was diluted in PBS to 20 ug/mL, coated onto 96-well plates (Nunc-Immuno #446612) at 100 μL/well, and incubated overnight at 4°C. Plates were washed once with 0.05% Tween20 in PBS (200 μL/well), followed by blocking for 2 hours at room temperature with 2% BSA in PBS (200 μL/well). Plates were again washed once with 0.05% Tween20 in PBS (200 μL/well). Serum samples from mice treated with Tat-PYC-Smad7 and mock gel were first diluted 1:6.25 (the lowest possible dilution), followed by serial dilutions up to 1:800. A Smad7 mouse monoclonal antibody (R&D #MAB2029) was first diluted to 2 μg/mL, followed by a one-third serial dilution. Serum sample dilutions and Smad7 antibody dilutions were added to plates at 50 μL/well and incubated for 2 hours at room temperature. Plates were washed twice with 0.1% Tween20 in PBS (200 μL/well). HRP-anti mouse IgG (Sigma #A4416) was diluted to 1:20,000 in 2% BSA-PBS and added to plates at 100 μL/well for 1 hour at room temperature. Plates were washed 6 times with 200 μL/well of 0.1% Tween20 in PBS. 1-Step Ultra TMB-ELISA (Thermo #34028) was added to plates at 50 μL/well and incubated at room temperature in the dark for 30 minutes; 50 μL/well of 2M sulfuric acid was added to plates. A microplate reader (Biotek synergy 2) was used to measure the optical density of each well at 450 nm, and OD 450 values were plotted in Graphpad Prism.

Statistical analysis

Ulcer incidence was analyzed by Fisher's exact test; differences between 2 treatment groups was determined using Student *t* test. Data are presented with each individual sample value or as the mean ± standard error of the mean.

Results

Establishing an IMRT-induced oral mucositis model in dogs

We first established IMRT-induced oral mucositis in dogs in a clinically relevant setting. We tested an IMRT dose of 20 to 30 Gy delivered in 5 fractions of 4 to 6 Gy targeted to the mucosa in the first 4 beagles. The irradiated mucosa began to show erythema the second week after initial RT (Fig. 1A, B), thus mock gel was applied daily from day 7 to day 19 (Fig. 1). The VRTOG scores show the grades and duration of gross damage were dose-related, with 6 Gy × 5 being the most severe (Fig. 1A,B). Histopathology of day 19 biopsies revealed that all 3 dosing protocols induced oral ulcers, with 6 Gy × 5 being the most severe in epithelial ablation and marked inflammation (Fig. E4). Mandible

mucosa had more epithelial ablation than maxillary mucosa in dog 3 (see Fig. E4), whereas the left and right sides of maxillary mucosa in dog 4 were similar in VRTOG scores (Fig. 1B) and in histopathology severity in ulceration, inflammation, and epithelial ablation (Fig. 2A). Clinical chemistry and hematology tests did not show consistent abnormalities (Supplementary Clinical Data), indicating the damage was largely restricted to local lesions.

Tat-PYC-Smad7 treatment reduced oral mucositis severity in dogs

Based on these findings, we chose the 5 Gy × 5 IMRT regimen to test Tat-PYC-Smad7 oral gel treatment at the maxillary mucosa, starting on day 8 after initial irradiation. Maxilla biopsies from dogs treated with mock oral gel only were used as the vehicle control for histopathology and pharmacological dynamic markers, except dog 2, in which the epithelium was completely ablated. We mimicked a "time-to-event continual reassessment method" of phase 1 radiation trials in human patients[22,23] for our dose-finding experiments. This design is adaptive and provides close estimates for maximal tolerated dose. The remaining 6 dogs were treated with Tat-PYC-Smad7, 0.5 to 8 μg daily dose, in 0.5 mL oral gel to cover the irradiated area. To confirm rapid drug-specific cell entry, we included an additional 8 μg dose of Tat-PYC-Smad7-HA protein (with the HA tag added to the c-terminal Tat-PYC-Smad7 protein), to allow HA-specific immunostaining. Among dogs exposed to 5 Gy × 5 RT in the maxilla, although there are individual variations in VRTOG scores, compared to mock gel treated dogs (with 0.5 μg or without Tat-PYC-Smad7 treatment in neighboring mucosa), grade 3 scores were significantly shortened by Tat-PYC-Smad7 treatments, from 8.75 ± 1.5 days to 4.16 ± 2.3 days (Fig. 1B,C). With the exception of the 0.5 μg dose, in which the treated side had a much shorter grade 3 score than vehicle treated side (Fig. 1D), other treatment dogs had no ulceration in Tat-PYC-Smad7 treated and neighboring sites (Fig. 1B), suggesting a bystander or systemic effect of Tat-PYC-Smad7 treatment with doses >0.5 μg/day. The dose-dependence of Tat-PYC-Smad7 was not obvious, but gross scores for all doses of Tat-PYC-Smad7 were better than vehicle treatment in the 5 Gy × 5 RT regimen. These data suggest a range of effective doses, and the maximal tolerated dose was not reached.

Histopathology demonstrated that all irradiated mucosa treated with mock gel only and mock gel treated mucosa adjacent to the 0.5 μg dose of Tat-PYC-Smad7 developed ulceration with marked inflammation (n = 4) (Fig. 2A). Tat-PYC-Smad7 treated mucosa post-RT did not harbor ulceration, and inflammation was relatively mild (except 1 dog with 8 μg dose) in comparison with either vehicle treated mucosa or their own pre-RT biopsies in normal mucosa (n = 6) (Fig. 2B). The lowest dose (0.5 μg) had a small area of epithelial thinning and erosion that was not seen in higher doses. These differences in rates of ulceration comparing mock gel to all doses of Tat-PYC-Smad7 treated mucosa were statistically significant (Fig. 2C).

We performed Ki67 immunostaining to determine whether the thicker epithelium observed in Tat-PYC treated samples is due to keratinocyte proliferation, as we have observed in mouse models of oral mucositis treated with full-length Tat-Smad7 protein.[15,17] Indeed, Tat-PYC-Smad7 treated epithelium harbored higher rates of proliferation than mock gel treated epithelium (Fig. 2D,E). To confirm that Tat-PYC-Smad7 oral gel can rapidly enter

damaged mucosa, we used biopsy tissue treated with an 8 μg daily dose of Tat-PYC-Smad7-HA to perform HA tag specific immunostaining to detect our delivered protein and not endogenous Smad7. The final treatment was 30 minutes prior to biopsy. HA immunostaining demonstrated that Tat-PYC-Smad7-HA is largely located inside the cytosol or nucleus of barrier-compromised epithelial cells, whereas the mock gel treated site did not show significant staining (Fig. 3A). These results indicate either no immediate Tat-PYC-Smad7 crossover from the treatment side to the mock gel side or that the amount was below the detectable level.

Tat-PYC-Smad7 local application primarily targeted local tissue without eliciting anti-drug antibody against itself

Because the mock gel treated site with neighboring Tat-PYC-Smad7 doses higher than 0.5 μg also showed less severe pathologic alterations compared to mock gel only treated animals, we performed IHC to determine if Tat-PYC-Smad7 could cross over to the neighboring vehicle site. Tat-PYC-Smad7 was primarily identified at the treatment mucosal layers (Fig. 3A). To determine if locally applied Tat-PYC-Smad7 enters the bloodstream, thus causing systemic therapeutic effects in the neighboring vehicle site, we developed a Smad7 ELISA assay. We spiked Tat-PYC-Smad7 into untreated dog serum to establish a standard curve that detects Tat-PYC-Smad7 levels as low as 0.16 ng/mL. We compared Smad7 levels in dog serum samples before and after Tat-PYC-Smad7, with the last treatment 30 minutes before serum collection. Tat-PYC-Smad7 was not detected in the serum samples of dogs with any Tat-PYC-Smad7 doses (Fig. 3B). Therefore, the therapeutic effect of Tat-PYC-Smad7 was primarily local. To determine if Tat-PYC-Smad7 elicits anti-drug antibody (ADA) that would neutralize its therapeutic effects, we established Smad7 ADA ELISA. None of the dogs with Tat-PYC-Smad7 doses showed ADA (Fig. 3C).

Topical Tat-PYC-Smad7 treatment site had molecular changes associated with reduced inflammation, increased DNA repair, and cell survival/proliferation

To examine on-target effects of Tat-PYC-Smad7, we profiled molecular changes in biopsies treated with Tat-PYC-Smad7 or mock gel controls, using NanoString nCounter Canine IO Panel. Due to the limited number of treated dogs, biopsies from Tat-PYC-Smad7 treated mucosa at various doses (0.5–8 μg) were compared with vehicle treated biopsies (Fig. 4). This analysis of 800 genes in 12 samples (Table E1) identified 193 differentially expressed genes comparing Tat-PYC-Smad7 treated samples versus vehicle treated samples, with 152 genes more highly expressed in vehicle treated samples and 41 genes more highly expressed in Tat-PYC-Smad7 treated samples (Fig. E5A). Expression of reference genes was equally distributed (Fig. E5B). Examination of the relative expression of genes in each functional category revealed that most immune cell–related categories (eg, antigen presentation, complement, costimulatory signaling, secreted cytokines and chemokines, immune cell adhesion, JAK-STAT signaling, and interferon signaling) contained many more significantly downregulated genes in Tat-PYC-Smad7 treated samples (Fig. E5C).

Although few genes are present in other categories because of this gene panel’s focus, categories such as cell proliferation, DNA damage repair, matrix remodeling, and MAPK signaling were upregulated in TAT-PYC-Smad7 treated samples (see Fig. E5C). Gene set

enrichment analysis of this dataset (including the normalized expression of all 800 genes in 6 Tat-PYC-Smad7 treated samples vs the 6 vehicle treated samples) against these 28 gene sets identified a few modestly enriched pathways in Tat-PYC-Smad7 treated samples versus vehicle treated samples (likely due to the 800 gene focus of this panel rather than the approximately 19,000 gene canine transcriptome). NF-κB signaling and secreted cytokines and chemokines were enriched in vehicle treated samples, whereas cell proliferation, DNA damage repair, and MAPK signaling were enriched in Tat-PYC-Smad7 treated samples (Fig. 4A–F). It is noteworthy that these pathways include higher levels of pro-growth genes *CCND1*, *EGFR*, *ERBB2*, *ERBB3*, and *TP63* and lower levels of growth inhibitory *SMAD3* and *TGFB1* in Tat-PYC-SMAD7 treated samples (Fig. 4D–F). Many genes involved in NFκB signaling and secreted cytokines and chemokines, including *IL6*, *CCL2*, *CCL7*, *CCL8*, and *CCL20*, were decreased in Tat-PYC-Smad7 treated samples (Fig. 4B,C,G), suggesting decreased levels of inflammatory signaling in Tat-PYC-Smad7 treated samples. Together, these data suggest increased epithelial programming and decreased inflammation in the mucositis samples treated with Tat-PYC-Smad7.

Consistent with reduction in TNF/NFκB signaling found in NanoString analyses, IHC show that nuclear NFκB-p50^{+} cells, a marker of NFκB pathway activation, were significantly reduced in oral mucositis lesions treated with Tat-PYC-Smad7 compared to mock gel treatment (Fig. 5). Further, pSmad3^{+} cells, a marker of TGF-β pathway activation, were reduced with Tat-PYC-Smad7 treatment (Fig. 5). Correlated with an increased DNA repair signature in Tat-PYC-Smad7 treated lesions (Fig. 4C), cells positive for pH2AX foci, a marker for unresolved DNA damage by RT, were significantly reduced by Tat-PYC-Smad7 treatment (Fig. 5). Consistent with molecular signatures of reduced inflammation, MPO+ neutrophils were reduced by Tat-PYC-Smad7 treatment (Fig. 5). These results are similar to those observed in mouse models of oral mucositis treated with full length Tat-Smad7.[15,17]

Because a group of inflammatory cytokines downstream of NFκB and/or TGF-β were highly expressed in oral mucositis lesions (Fig. 4G), we used IHC to visualize their spatial patterns in the lesions. IL-1β, TNF-α, CCL2, and IL-6 were not detected in oral mucosa prior to RT (not shown), but these cytokines were detected in both oral epithelial cells and stromal cells after RT and were less prominent in Tat-PYC-Smad7 treated samples compared to vehicle (Fig. 6A). We sought to determine if these cytokines are secreted into the blood stream. Among them, TNF-α and IL-1β were significantly reduced, and IL-6 and CCL2 were trending lower in serum samples of dogs treated with local Tat-PYC-Smad7 treatment in comparison with serum samples of dogs treated with mock gel (Fig. 6B). Together, these data suggest local and systemic reductions of inflammatory cytokines/chemokines in irradiated dogs treated with Tat-PYC-Smad7.

Discussion

Canine oral mucositis model provides a tool for assessing therapeutic interventions

We established a clinically relevant canine oral mucositis model, which will provide a tool to screen and evaluate therapeutic interventions for oral mucositis in both canine and human oncology clinics. Unlike cancer lesions, biopsy of naturally occurring oral mucositis to evaluate pathology and possible drug targets is nearly impossible in human patients,

who experience tremendous pain from the lesions. Therefore, without a clinically relevant model, therapeutic interventions would largely depend on population observations. In our model, oral mucositis severity is largely comparable among dogs of different sexes and ages, although a larger number of subjects is needed to reveal a gender/age difference in oral mucositis susceptibility. With respect to location susceptibility to oral mucositis, in 1 dog exposed to the same RT dose, we observed more severe inflammation and epithelial ablation on the mandible mucosa than on the maxillary mucosa. Although we could not rule out the possibility of individual variation, our observation will instigate future clinical assessment of oral mucositis susceptibility among different mucosa locations so that therapeutic RT dose can be taken into consideration.

Tat-PYC-Smad7 topical application targets local cellular and molecular events associated with oral mucositis pathogenesis and provides potential systemic pharmacodynamics markers

Consistent with the cell penetration property of the Tat peptide upon direct contact, we detected Tat-PYC-Smad7 primarily in treated oral epithelial layers, with the highest levels in the surface damaged epithelial cells (Fig. 3A), similar to what was observed previously using full-length Tat-Smad7 in a mouse model of oral mucositis.[15] The local effects of Tat-PYC-Smad7 were apparent by markers of reduced DNA damage and reduced NFκB/TGFβ signaling at the site of application, consistent with previous studies demonstrating that the functional domains of PYC-SMAD7 recruit the ATM complex to sites of DNA damage to accelerate DNA repair[19] and bind to TAB2/TAB3 to disrupt NFκB activation,[18] in addition to the well-described role in attenuating TGF-β signaling. This could explain the direct local therapeutic effects and molecular targeting. However, in dogs treated with daily doses higher than 0.5 μg Tat-PYC-Smad7, we also saw improvement of the neighboring vehicle site in comparison with dogs treated with vehicle only. Because Tat-PYC-Smad7 was not detected at the systemic level, it is unlikely that Tat-PYC-Smad7 directly provided a systemic effect on the vehicle site. Given a broad effective dose range (0.5–8 μg daily dose), we could not rule out that crossover Tat-PYC-Smad7 into the neighboring vehicle site, even below a detectable level, could have a therapeutic effect.

An alternate explanation, based on our finding that inflammatory cytokines were lower in the blood of Tat-PYC-Smad7 treated dogs, is that systemic reduction provides an indirect systemic or bystander effect on the neighboring vehicle site. Although it can be argued whether these inflammatory cytokines were secreted from oral epithelial cells or from leukocytes that circulated from the oral mucositis back to the blood, we did not observe consistently elevated systemic neutrophils (Supplementary Clinical Data) in vehicle treated dogs as seen in oral mucositis lesions (Fig. 5). This is not surprising because most neutrophils die onsite.

Additionally, NanoString profiling in oral mucosal biopsies showed that transcriptional levels of these inflammatory cytokines correlated with protein levels. Most of these inflammatory cytokines are direct targets of NFκB and/or TGF-β signaling. Taken together, our data support the idea that systemic cytokine reduction by local Tat-PYC-Smad7 treatment is a consequence of its local targeting to epithelial cells to reduce secretion of

these cytokines or accelerate healing, thereby attenuating the secretion of these cytokines. These data have 2 potential implications for clinical interventions. First, given that it is almost impossible to biopsy oral mucositis lesions to examine pharmacodynamics markers, systemic cytokines downstream of NFκB and/or TGF-β could serve as indirect pharmacodynamics markers. Second, local Tat-PYC-Smad7 treatment of oral mucositis may not need to completely cover all lesions, particularly in locations where local coating is difficult, because bystander/indirect systemic therapeutic effects could alleviate those lesions.

Lack of systemic Tat-PYC-Smad7 via topical application and ADA provide safety advantages over systemic drugs in treating oral mucositis

As expected, Tat-PYC-Smad7 is primarily detected in epithelial cells, the initial point of contact for protein exposure. When epithelial layers are lost in ulcerated lesions, stromal cells would be exposed to Tat-PYC-Smad7. Although Tat-PYC-Smad7 transduction in these cells is part of the mechanism of its therapeutic effects, Tat-mediated cell penetration could potentially allow Tat-PYC-Smad7 to enter vessels in ulcerated lesions to reach systemic levels. We did not detect systemic Tat-PYC-Smad7 (Fig. 3B), possibly due to the combination of its rapid entry to local cells and the low effective doses. Therefore, compared to current systemic delivery of treatments in development, local Tat-PYC-Smad7 application could have safety advantages. Future toxicology studies require intentional systemic exposure to larger doses to fully assess safety, but the current study provides a platform for measurement of systemic exposure. Another safety concern for any protein drug is the potential to elicit ADAs, which would neutralize/block the protein drug effect and potentially cross react with endogenous Smad7, thus affecting its physiologic functions. We did not detect ADA in dogs with any dose of Tat-PYC-Smad7 (Fig. 3C). This could be because both Tat peptide and Smad7 protein have low immunogenicity and the treatment period is relatively short. Because oral mucositis treatment is expected to be short, it adds an additional safety margin.

Conclusions

Our current study provides a novel model to assess therapeutic interventions for oral mucositis readily applicable to the veterinary oncology clinic and provides experimental data for therapeutic development in human oral mucositis patients. We demonstrated feasibility, mechanism of actions, and safety assessment of Tat-PYC-Smad7 in treating oral mucositis through local application. Our studies also established tools for clinical pharmacology/toxicology studies of Tat-PYC-Smad7 to be used as a novel drug to treat oral mucositis.

Supplementary Material

Refer to Web version on PubMed Central for supplementary material.

Acknowledgements

The authors Nicole Manning for assistance with sectioning tissue blocks for this project and Pamela Garl for proofreading this manuscript.

This study was supported by grants from the National Institutes of Health (R44DE024659 and R44DE028718) and by philanthropy from an anonymous donor for the Head and Neck Cancer Research Program.

References

1. Sonis ST. Oral mucositis in head and neck cancer: Risk, biology, and management. ASCO Am Soc Clin Oncol Meeting 2013;2013:236–240.
2. Villa A, Sonis ST. Mucositis: Pathobiology and management. Curr Opin Oncol 2015;27:159–164. [PubMed: 25774860]
3. Grier CK, Mayer MN. Radiation therapy of canine nontonsillar squamous cell carcinoma. Can Vet J 2007;48:1189–1191. [PubMed: 18050803]
4. Rejec A, Benoit J, Tutt C, Crossley D, Butinar J, Hren NI. Evaluation of an accelerated chemoradiotherapy protocol for oropharyngeal squamous cell carcinoma in 5 cats and 3 dogs. J Vet Dent 2015;32:212–221. [PubMed: 27012058]
5. Mosca A, Gibson D, Mason SL, Dobson J, Giuliano A. A possible role of coarse fractionated radiotherapy in the management of gingival squamous cell carcinoma in dogs: A retrospective study of 21 cases from two referral centers in the uk. J Vet Med Sci 2021;83:447–455. [PubMed: 33487622]
6. Khuntia D, Harris J, Bentzen SM, et al. Increased oral mucositis after IMRT versus non- when combined with cetuximab and cisplatin or docetaxel for head and neck cancer: Preliminary results of RTOG 0234. Int J Radiat Oncol Biol Phys 2008;72.
7. Al-Dasooqi N, Sonis ST, Bowen JM, et al. Emerging evidence on the pathobiology of mucositis. Support Care Cancer 2013;21:2075–2083. [PubMed: 23604521]
8. Sonis ST. Efficacy of palifermin (keratinocyte growth factor-1) in the amelioration of oral mucositis. Core Evid 2010;4:199–205. [PubMed: 20694076]
9. Sonis ST. The pathobiology of mucositis. Nat Rev Cancer 2004;4:277–284 Core Evid. 2010;4:199–205. [PubMed: 15057287]
10. Collen EB, Mayer MN. Acute oropharyngeal effects of full-course radiation treatment of tumors of the head. Can Vet J 2008;49:509–512. [PubMed: 18512465]
11. Sa G, Xiong X, Wu T, Yang J, He S, Zhao Y. Histological features of oral epithelium in seven animal species: As a reference for selecting animal models. Eur J Pharm Sci 2016;81:10–17. [PubMed: 26432596]
12. Henke M, Alfonsi M, Foa P, et al. Palifermin decreases severe oral mucositis of patients undergoing postoperative radiochemotherapy for head and neck cancer: A randomized, placebo-controlled trial. J Clin Oncol 2011;29:2815–2820. [PubMed: 21670447]
13. Le QT, Kim HE, Schneider CJ, et al. Palifermin reduces severe mucositis in definitive chemoradiotherapy of locally advanced head and neck cancer: A randomized, placebo-controlled study. J Clin Oncol 2011;29:2808–2814. [PubMed: 21670453]
14. Anderson CM, Sonis ST, Lee CM, et al. Phase 1b/2a trial of the superoxide dismutase mimetic GC4419 to reduce chemoradiotherapy-induced oral mucositis in patients with oral cavity or oropharyngeal carcinoma. Int J Radiat Oncol Biol Phys 2018;100:427–435. [PubMed: 29174131]
15. Han G, Bian L, Li F, et al. Preventive and therapeutic effects of smad7 on radiation-induced oral mucositis. Nat Med 2013;19:421–428. [PubMed: 23475202]
16. Lu SL, Reh D, Li AG, et al. Overexpression of transforming growth factor beta1 in head and neck epithelia results in inflammation, angiogenesis, and epithelial hyperproliferation. Cancer Res 2004;64:4405–4410. [PubMed: 15231647]
17. Luo J, Bian L, Blevins MA, et al. Smad7 promotes healing of radiotherapy-induced oral mucositis without compromising oral cancer therapy in a xenograft mouse model. Clin Cancer Res 2019;25:808–818. [PubMed: 30185419]
18. Hong S, Lim S, Li AG, et al. Smad7 binds to the adaptors TAB2 and TAB3 to block recruitment of the kinase TAK1 to the adaptor TRAF2. NatImmunol 2007;8:504–513.
19. Park S, Kang JM, Kim SJ, et al. Smad7 enhances ATM activity by facilitating the interaction between ATM and Mre11-Rad50-Nbs1 complex in DNA double-strand break repair. Cell Mol Life Sci 2015;72:583–596. [PubMed: 25063542]

20. Reis PP, Waldron L, Goswami RS, et al. mRNA transcript quantification in archival samples using multiplexed, color-coded probes. BMC Biotechnol 2011;11:46. [PubMed: 21549012]
21. Norton N, Sun Z, Asmann YW, et al. Gene expression, single nucleotide variant and fusion transcript discovery in archival material from breast tumors. PLoS One 2013;8:e81925. [PubMed: 24278466]
22. Normolle D, Lawrence T. Designing dose-escalation trials with late-onset toxicities using the time-to-event continual reassessment method. J Clin Oncol 2006;24:4426–4433. [PubMed: 16983110]
23. Polley MY. Practical modifications to the time-to-event continual reassessment method for phase I cancer trials with fast patient accrual and late-onset toxicities. Stat Med 2011;30:2130–2143. [PubMed: 21590790]

A

VRTOG Grade	0	1	2	3
Appearance	No change over baseline	Erythema No mucositis	Patchy mucositis Seemingly pain-free	Confluent fibrinous mucositis, ulceration, necrosis, hemorrhage

Grade 0
Grade 1
Grade 2
Grade 3

B

Tat-PYC-Smad7, daily 7-12, 15-19

Day	0 Age/Sex	1-5 RT*	6	7	8	9	10	11	12	13	14	15	16	17	18	19	20	21	22	23	24	25	26	27	28	29	30
Dog 1, L Mock gel	3yr/f	4Gyr5														U											
Dog2, R Mock gel	3yr/f	6Gyx5														U											
Dog3, R Mock gel	4yr/f	5Gyx5														U											
Dog4, L Mock gel	4yr/M	5Gyx5														U											
Dog4, R Mock gel	4yr/M	5Gyx5														U											
Dog9, L Mock gel	2.5yr/F	5Gyx5														U											
Dog9, R 0.5ug	2.5yr/F	5Gyx5														N											
Dog5, L 1ug	3.5yr/M	5Gyx5														N											
Dog6, L 2ug	3yr/M	5Gyx5														N											
Dog7, L 4ug	4yr/M	5Gyx5														N											
Dog8, R 8ug	2.5yr/F	5Gyx5														N											
Dog10, L 8ug	2.5yr/F	5Gyx5														N											

*: Maxilla irradiation; L: Left; R: Right; U: ulceration; N: no ulceration

C

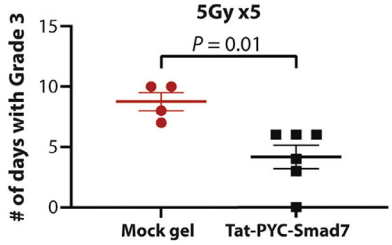

D

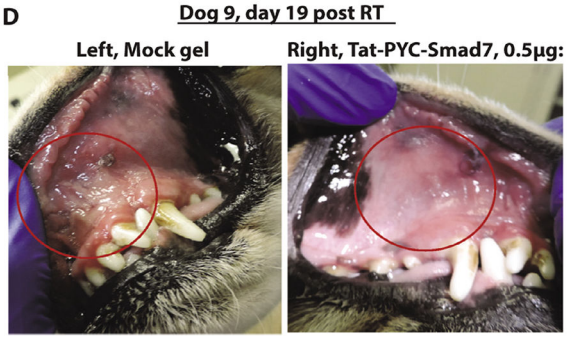

Fig. 1.

Gross scores and appearance of Tat-PYC-Smad7 treatment in dog oral mucositis. (A) Veterinary Radiation Therapy Oncology Group grade criteria and color codes. (B) Gross scores of each dog over time. (C) Quantification of the number of days of grade 3 mucositis for each dog and the mean of each treatment ± standard error of the mean. (D) Maxilla mucosal images of dog 9 on the vehicle control side vs Tat-PYC-Smad7 treatment side on day 19 as an example of different gross scores. Red circles highlight irradiated areas.

Abbreviations: RT = radiation therapy; VROTG = Veterinary Radiation Therapy Oncology Group.

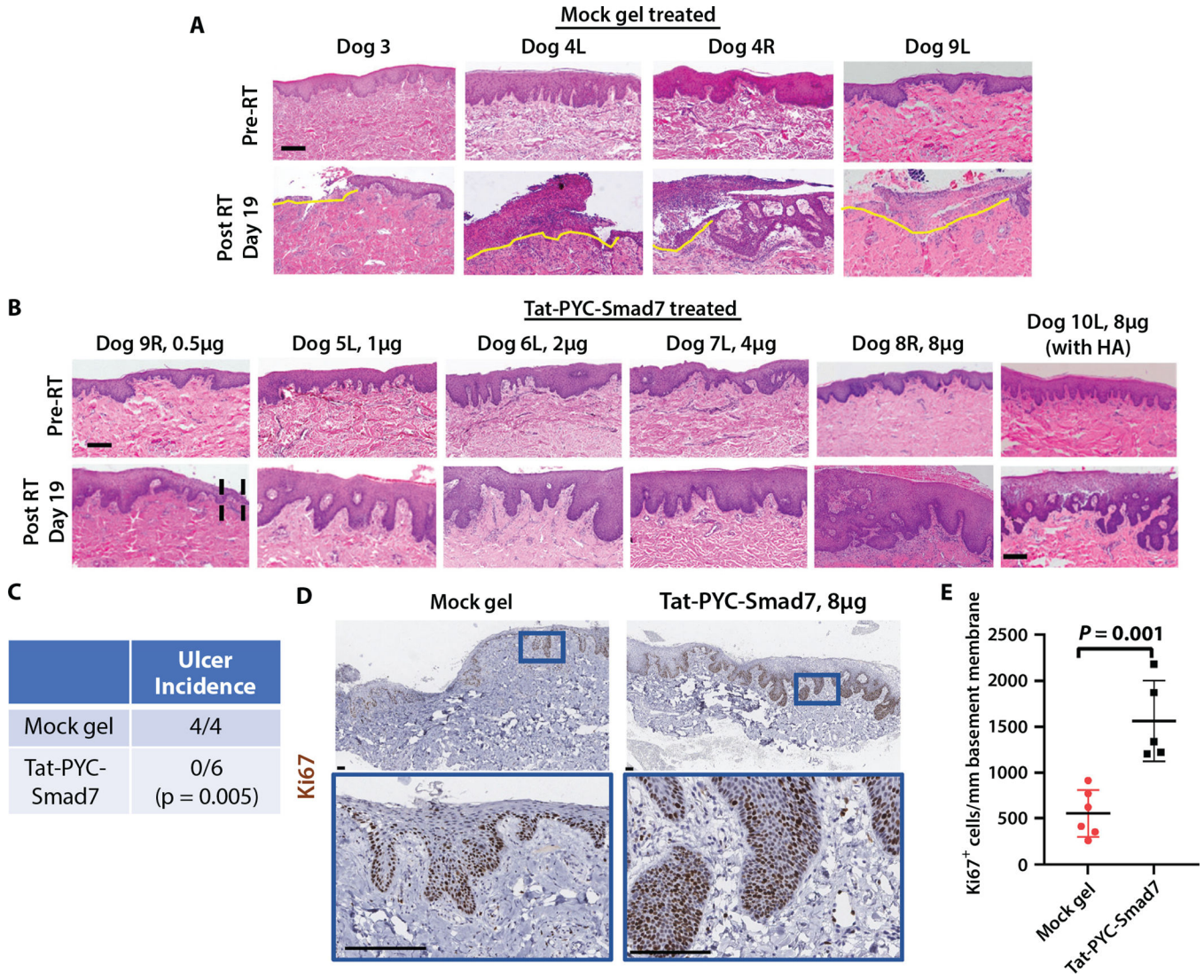

Fig. 2.

Histology of Tat-PYC-Smad7 treated dog mucositis. Biopsies from maxilla mucosa irradiated by 5 Gy × 5 intensity modulated radiation therapy. (A) Biopsies from mock gel treatment. L: left side from the midline; R: right side from the midline. Yellow lines delineate ulcers with epithelial ablation and massive infiltrated immune cells. Scale bar: 200 μm. (B) Biopsies from Tat-PYC-Smad7 treatments. Black dotted lines in 0.5 μg dose delineate epithelial thinning and erosion. The 8 μg dose induced the most hyperplasia compared to other doses, with one showing profound inflammation. Scale bar: 200 μm. (C) Quantification of ulcer incidence in each treatment group and statistical comparison by Fisher's exact test. (D) Ki67 immunohistochemistry to identify proliferating cells. Lower panels present high-power view of the blue box identified in the upper panels. Scale bar: 100 μm. (E) Quantification of $Ki67^+$ epithelial cells per millimeter epithelium for each dog and the mean of each treatment ± standard error of the mean. *Abbreviations*: HA = hemagglutinin; L = left; R = right; RT = radiation therapy.

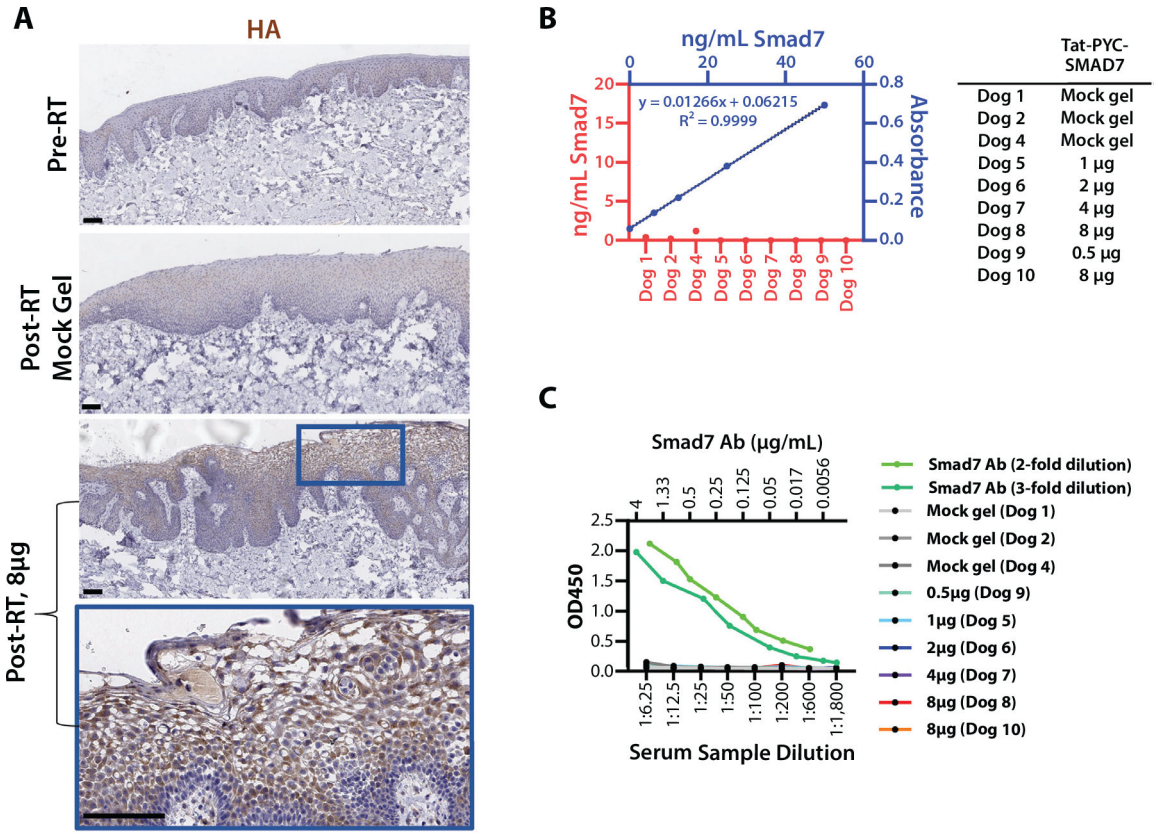

Fig. 3.

Tat-PYC-Smad7 targets local tissue. (A) Cell penetration of topical drug in RT irradiated oral mucosa. Antibody against c-terminal hemagglutinin tag was used for immunostaining. Lower panels present high-power view of the blue box identified in the panel above. Scale bar: 100 μm. (B) Tat-PYC-Smad7 was not detected in serum samples of topically treated dogs. The plasma of 2 untreated dogs diluted 1:4 was spiked with 0 to 50 ng/mL Tat-PYC-Smad7 protein to generate standard curves, which were averaged (presented in blue). The amount of Smad7 in the posttreatment plasma (diluted 1:4) was measured against the standard curves. (C) Lack of anti-drug antibody (ADA) against Tat-PYC-Smad7 from locally treated oral mucositis. Two independent assays (2 standard curves in light and dark green) for ADA examinations. No ADA against Tat-PYC-Smad7 was detected in dogs with oral mucosa Tat-PYC-Smad7 treatment for 2 weeks. *Abbreviation*: RT = radiation therapy.

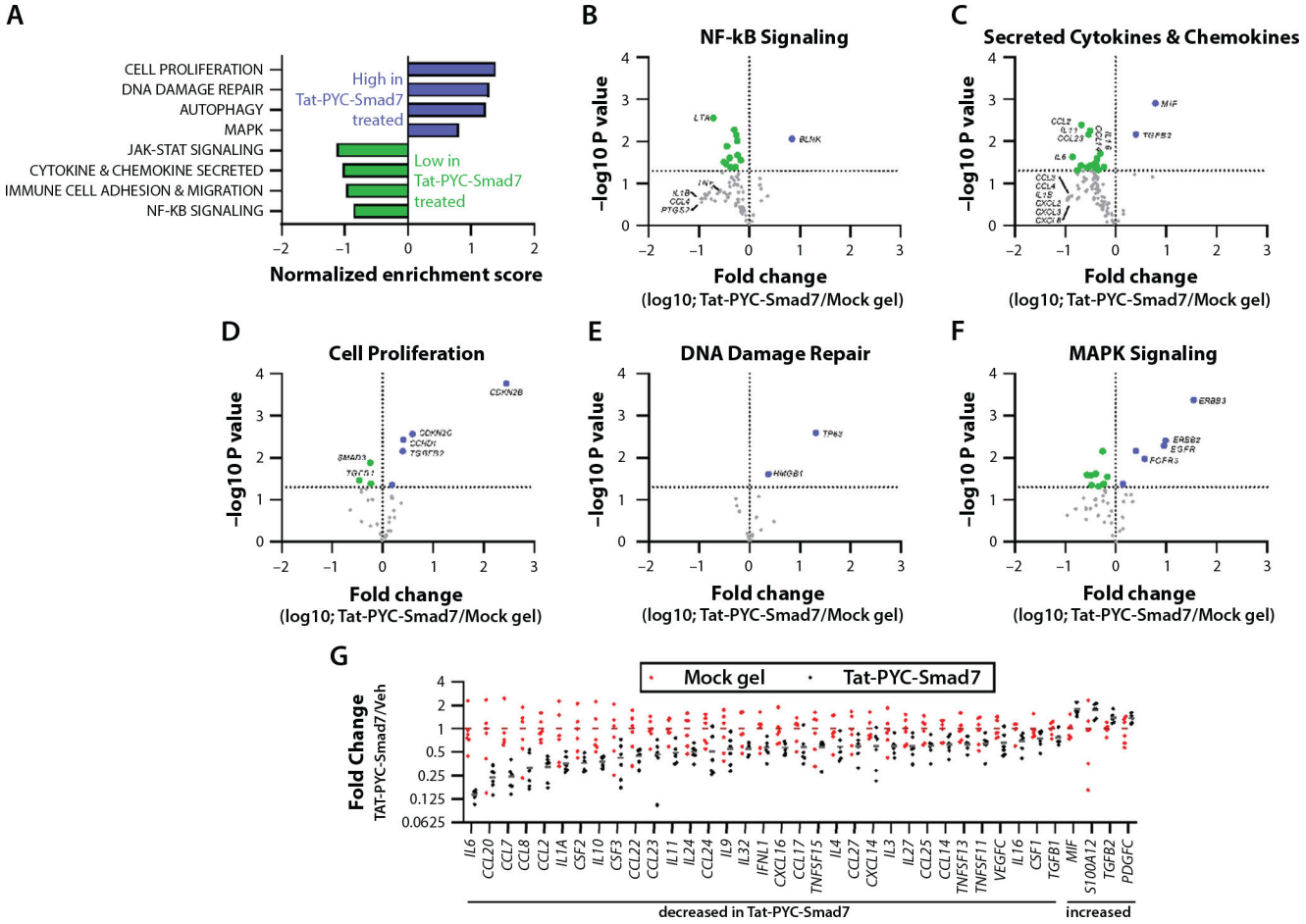

Fig. 4.

Genes and functional pathways altered in Tat-PYC-Smad7 treated samples. RNA harvested from formalin fixed, paraffin embedded biopsy samples (6 vehicle treated samples versus 6 Tat-PYC-Smad7 treated samples) was subjected to NanoString nCounter Canine IO panel analysis. (A) Relative gene expression in 28 functional categories was analyzed by gene set enrichment analysis. Categories enriched in Tat-PYC-Smad7 treated samples versus vehicle treated samples as determined by normalized enrichment scores are presented. (B-F) Volcano plots presenting the log10 transformed fold change (on the x axis) and the −log10 transformed *P* value (on the y axis) of individual genes comparing Tat-PYC-Smad7 to vehicle in 5 functional categories, with individual genes highlighted. Genes to the left of the vertical line (green) are decreased in Tat-PYC-Smad7 treated samples, and genes to the right of the vertical line (blue) are increased in Tat-PYC-Smad7 treated samples. The horizontal line indicates $P = .05$, and points above this line represent differences with $P < .05$. (G) The relative expression of all secreted chemokines and cytokines in each sample with a significant difference between vehicle and Tat-PYC-SMAD7 treatments ($P < .05$ as determined by 2-tailed Student *t* test) are presented.

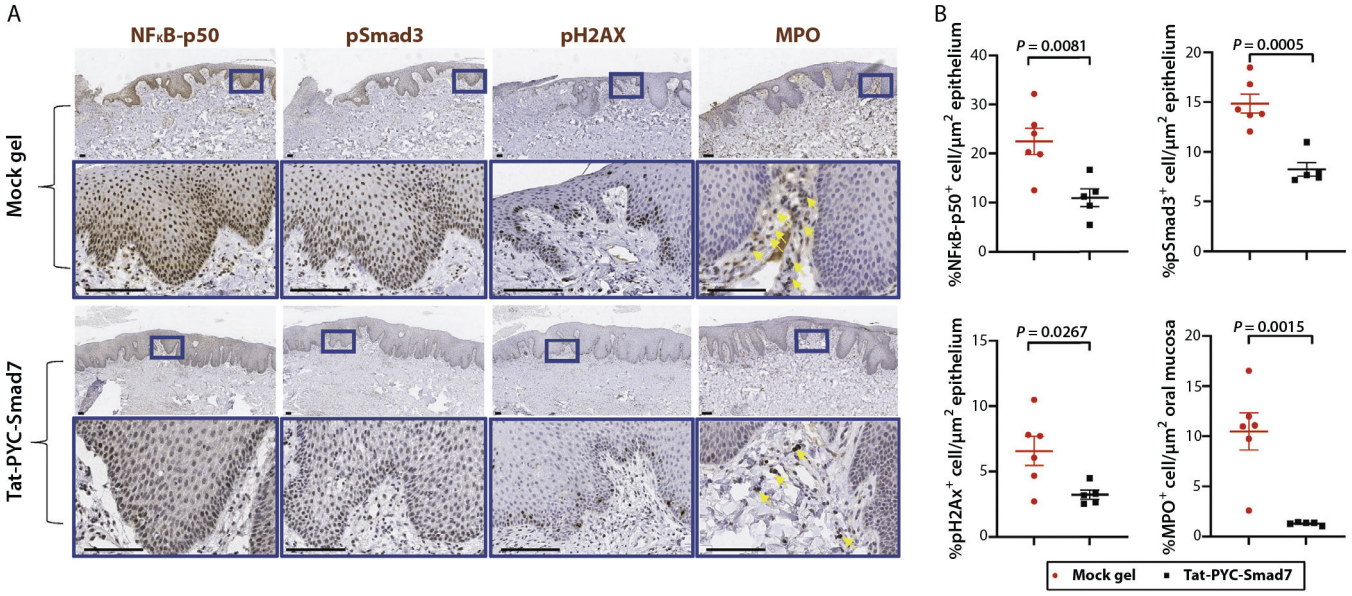

Fig. 5.

Pharmacodynamics markers of Tat-PYC-Smad7 treated dog oral mucositis. (A) Biopsies of posttreatment oral mucosa were evaluated by immunohistochemistry to detect NFkB-p50, pSmad3, pH2AX, and myeloperoxidase. Representative images of vehicle treated and Tat-PYC-Smad7 treated mucosa are presented with the lower panel in each set, presenting a high-power view of the blue box identified in the panel above. Scale bar: 100 μm. (B) Quantification of positive, brown-staining in epithelium sections excluding ulcers (in vehicle group) pictured in panel A. Myeloperoxidase staining together with morphology evaluation were used to identify neutrophils (indicated by yellow arrows) in ulcer surface and stroma. Faint brown staining in epithelium is nonspecific. The staining quantification for each dog and the mean of each treatment ± standard error of the mean is presented.

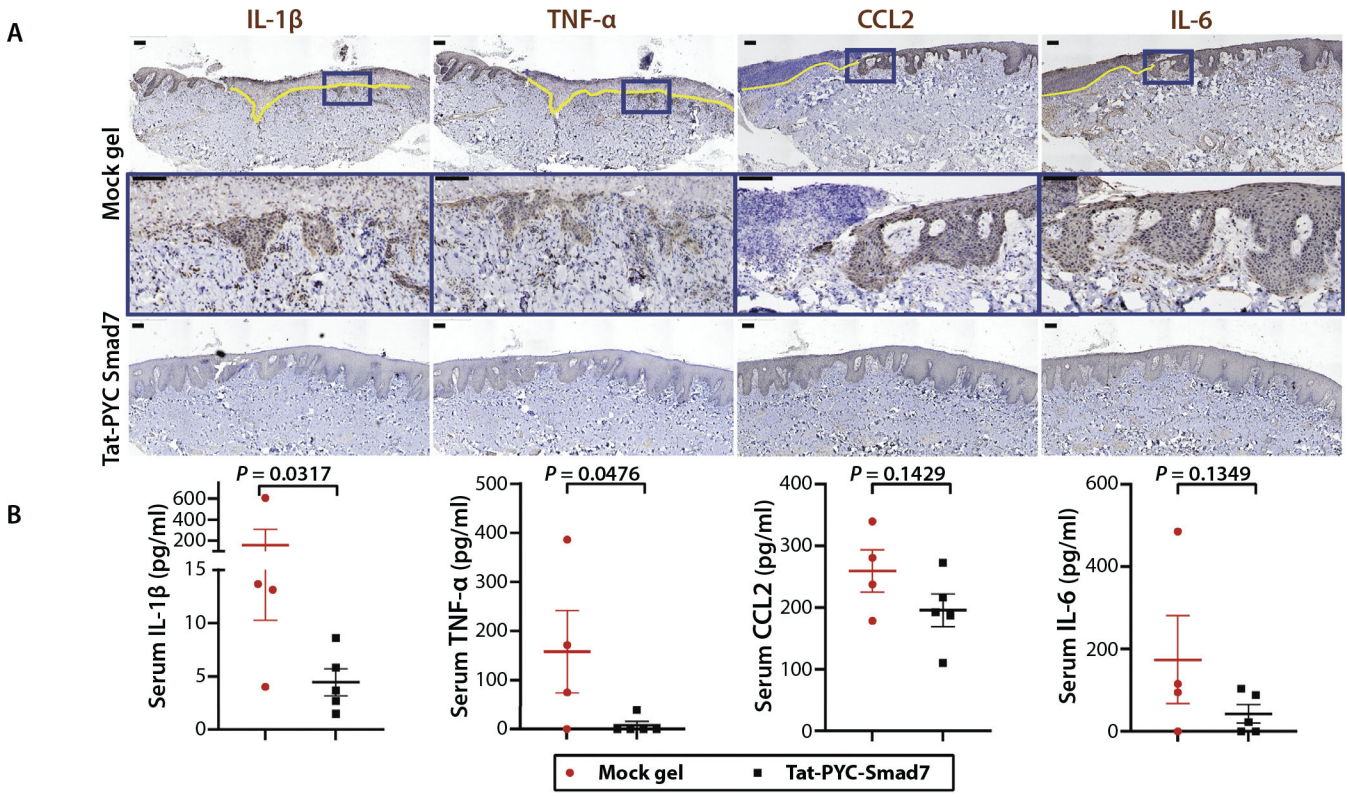

Fig. 6.

Tat-PYC-Smad7 reduced inflammatory cytokines released from oral mucositis lesions. (A) Immunohistochemistry showing inflammatory cytokines detected in mucosal epithelial and stromal cells. Yellow line highlights the ulcerated region. Insets (blue boxes) on top panels of vehicle group are enlarged in the panels below. Scale bar is 100 μm. (B) Serum detection of cytokines shown in A. Vehicle: mock gel from 4 dog biopsies with vehicle treatment only after radiation therapy; Tat-PYC-Smad7: from 5 dog biopsies treated with 1, 2, 4, and 8 μg daily dose of Tat-PYC-Smad7 treatment after radiation therapy. The serum quantification for each dog and the mean of each treatment ± standard error of the mean is presented.